

On the two-dimensional stability of the axisymmetric Burgers vortex

A. Prochazka and D. I. Pullin

Graduate Aeronautical Laboratories 205-45, California Institute of Technology, Pasadena, California 91125

(Received 28 December 1994; accepted 16 February 1995)

The stability of the axisymmetric Burgers vortex solution of the Navier–Stokes equations to two-dimensional perturbations is studied numerically up to Reynolds numbers, $R = \Gamma/2\pi\nu$, of order 10^4 . No unstable eigenmodes for azimuthal mode numbers $n = 1, \dots, 10$ are found in this range of Reynolds numbers. Increasing the Reynolds number has a stabilizing effect on the vortex. © 1995 American Institute of Physics.

Taylor¹ was the first to note the importance of the interaction of vortex stretching and viscosity to intensify and diffuse vorticity in the process of dissipating energy in turbulence. A solution to the Navier–Stokes equations that models this interaction was discovered by Burgers.² This has been used in turbulence applications by Townsend³ and others. Large-scale numerical simulations by She, Jackson, and Orszag,⁴ Vincent and Meneguzzi,⁵ and Jiménez *et al.*⁶ have indicated the presence of vortices whose characteristics resemble those of Burgers vortices. The stability of the Burgers vortex in both two and three dimensions is therefore of interest. This problem was studied analytically for low Reynolds numbers by Robinson and Saffman⁷ henceforth referred to as RS.

The problem will be formulated in the cylindrical polar coordinate system (r, θ, z) where the velocity field in the respective directions will be denoted by $\mathbf{u} = (u_r, u_\theta, u_z)$. This velocity field is decomposed as

$$u_r = -(\gamma/2)r + \hat{u}_r(r, \theta, t), \quad (1)$$

$$u_\theta = \hat{u}_\theta(r, \theta, t), \quad (2)$$

$$u_z = \gamma z, \quad (3)$$

where \hat{u}_r and \hat{u}_θ are the rotational part of the velocity field and γ is the rate of strain in the z direction corresponding to a uniform axisymmetric external strain. Substitution of (1)–(3) into the vorticity equation gives

$$\frac{\partial \omega}{\partial t} + u_r \frac{\partial \omega}{\partial r} + \frac{u_\theta}{r} \frac{\partial \omega}{\partial \theta} = \gamma \omega + \frac{\nu}{r} \left[\frac{\partial}{\partial r} \left(r \frac{\partial \omega}{\partial r} \right) + \frac{1}{r} \frac{\partial^2 \omega}{\partial \theta^2} \right], \quad (4)$$

where the vorticity field is nonzero only in the z direction $\omega = (0, 0, \omega)$. It is well known that a steady axisymmetric solution of (4) is given by

$$\omega_0(r) = (\gamma\Gamma/4\pi\nu)e^{-\gamma r^2/4\nu}, \quad (5)$$

which induces the angular velocity,

$$\hat{u}_{\theta 0} = (\Gamma/2\pi r)(1 - e^{-\gamma r^2/4\nu}), \quad (6)$$

where Γ is the total circulation. Equations (5)–(6) are the axisymmetric Burgers vortex and represent an equilibrium which is a balance between the stretching of vortex lines by the external strain and the lateral diffusion of vorticity.

While the stability of (5)–(6) to three-dimensional (3-D) perturbations is of fundamental interest, we presently consider the stability to two-dimensional (2-D) disturbances. All

quantities are nondimensionalized with respect to length scale $\sqrt{\nu/\gamma}$ and time scale γ^{-1} . The 2-D perturbed velocity field in the r - θ plane is

$$u_r = u_{r0} + u'_r(r, \theta, t), \quad u_\theta = u_{\theta 0} + u'_\theta(r, \theta, t), \quad (7)$$

$$\omega = \omega_0 + \omega'(r, \theta, t).$$

A perturbation streamfunction ψ' can be defined such that

$$u'_r = \frac{1}{r} \frac{\partial \psi'}{\partial \theta}, \quad u'_\theta = -\frac{\partial \psi'}{\partial r}, \quad (8)$$

$$\nabla^2 \psi' = -\omega'. \quad (9)$$

The perturbations are assumed to be of the normal mode form

$$\omega' = \omega(r)e^{-\mu t + in\theta}, \quad (10)$$

$$\psi' = \psi(r)e^{-\mu t + in\theta}, \quad (11)$$

where n is the azimuthal mode and $-\mu$ is the complex growth rate of the perturbation. In this formulation, unstable solutions correspond to negative values of the real part of μ . Using (8)–(11) in (4) and linearizing, it is found that

$$L^n \omega + \mu \omega = inR(-f\psi + \frac{1}{2}g\omega), \quad (12)$$

$$M^n \psi = -\omega, \quad (13)$$

where $R = \Gamma/2\pi\nu$ is a Reynolds number, the primes on the perturbation variables have been dropped for convenience, and

$$M^n(\cdot) \equiv \frac{1}{r} \frac{d}{dr} \left(r \frac{d}{dr} (\cdot) \right) - \frac{n^2}{r^2} (\cdot), \quad (14)$$

$$L^n(\cdot) \equiv M^n(\cdot) + \frac{1}{r} \frac{d}{dr} [r^2(\cdot)], \quad (15)$$

$$f \equiv e^{-r^2/2}, \quad g \equiv (1 - e^{-r^2/2})/(r^2/2). \quad (16)$$

The first part of the RS analysis dealt with the special case of $R=0$; the Stokes limit of (1)–(4) with the present scaling. Solutions were found in terms of the confluent hypergeometric function and, enforcing exponential decay at infinity, gave eigenvalues $\mu = n + 2k$, $k=0, 1, 2, \dots$. Since the eigenvalues are all positive real, the Burgers vortex is stable for zero circulation. The $R=0$ normalized vorticity eigenfunctions are

$$\omega(n,k) = 2^{-n/2} r^n e^{-r^2/2} L_k^{(n)}(r^2/2). \quad (17)$$

The streamfunction eigenfunctions can be found by integrating the vorticity eigenfunctions to give

$$\psi(r;n,0) = \frac{1}{2} [\Gamma(n)/(r^2/2)^{n/2}] [1 - e_{n-1}(r^2/2)e^{-r^2/2}], \quad (18)$$

$$\psi(r;n,k) = (1/2k) r^n e^{-r^2/2} L_{k-1}^{(n)}(r^2/2), \quad (19)$$

where e_{n-1} is the exponential series truncated after $n-1$ terms.

In order to tackle the problem numerically, we first obtain from (12)–(13) one equation for the vorticity,

$$\mathcal{L}(\omega) = -\mu\omega, \quad (20)$$

which is a complex eigenvalue problem with

$$\mathcal{L}(\cdot) = L^n(\cdot) - i n R [f(M^n)^{-1}(\cdot) + \frac{1}{2} g(\cdot)]. \quad (21)$$

The behavior at the boundaries for the finite Reynolds number problem is identical to that found for the $R=0$ case. Using boundedness of solutions and a Frobenius method about the regular singular point, $r=0$, we find the behavior of the vorticity to be,

$$\omega = O(r^n), \quad r \rightarrow 0. \quad (22)$$

For $r \rightarrow \infty$, a dominant balance argument is used to write Eq. (20) as

$$\frac{1}{r} \frac{d}{dr} \left(r \frac{d}{dr} \omega \right) - \frac{n^2}{r^2} \omega + \frac{1}{r} \frac{d}{dr} [r^2 \omega] + \mu \omega = \frac{i n R \omega}{r^2}, \quad (23)$$

which can be written simply as

$$L^{(n^2 + \ln R)^{1/2}}(\omega) + \mu \omega = 0, \quad (24)$$

so that the behavior at infinity remains the same as for $R=0$,

$$\omega \sim A r^\mu e^{-r^2/2}, \quad r \rightarrow \infty. \quad (25)$$

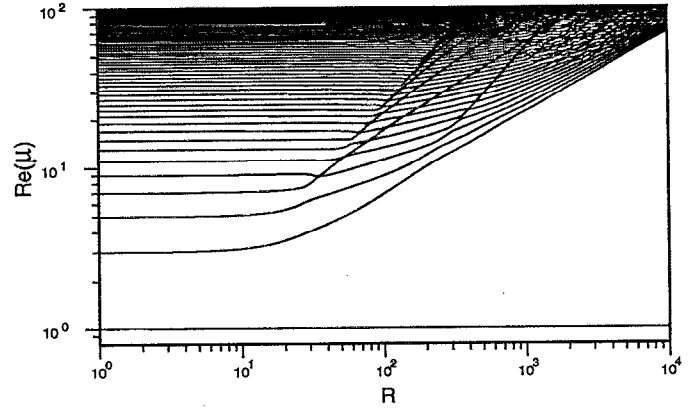


FIG. 1. Real part of the eigenvalues versus Reynolds number for $n=1$, $N=300$, $k=0,1,2,\dots$ defined by the y axis intercept, $n+2k$.

A Galerkin approach was used to expand solutions in the orthogonal basis defined by the $R=0$ vorticity eigenfunctions

$$\omega = \sum_{k=0}^{N-1} a_k \omega(r;n,k), \quad \omega(r;n,k) = 2^{-n/2} r^n e^{-r^2/2} L_k^{(n)}\left(\frac{r^2}{2}\right), \quad (26)$$

where the finite expansion is truncated at $N-1$ terms. Substitution of (26) into (20) results in a complex eigenvalue problem of the form

$$\mathbf{A} \mathbf{x} = -\mu \mathbf{x}, \quad (27)$$

where $\mathbf{x} = (a_0, a_1, \dots, a_{N-1})^T$ and \mathbf{A} is complex matrix of order $N \times N$ whose coefficients are found by using the orthogonality of the basis functions under the weighted inner product,

TABLE I. Comparison with Robinson and Saffman's results for small Reynolds number, $N=50$, and $\mu = \mu_0 + R\mu_1 + R^2\mu_2$.

n	k	$-i\mu_1$ (RS)	$-i\mu_1$	$10^2\mu_2$ (RS)	$10^2\mu_2$
1	0	0	0.000 000 00	0	0.000 000 00
1	1	0.125	0.124 999 77	0.144 350 71	0.144 350 55
1	2	0.125	0.125 000 03	0.100 947 94	0.100 948 33
⋮	⋮	⋮	⋮	⋮	⋮
1	7	0.091 644 3	0.091 642 55	0.002 259 61	0.002 259 88
1	8	0.087 280 3	0.087 281 27	-0.000 431 672	-0.000 433 45
1	9	0.083 461 8	0.083 466 71	-0.002 078 14	-0.002 077 72
2	0	0.025	0.024 999 94	0.278 558 29	0.278 555 88
2	1	0.025	0.024 999 94	0.427 980 57	0.427 983 54
2	2	0.023 437 5	0.023 437 52	0.026 361 97	0.026 362 17
⋮	⋮	⋮	⋮	⋮	⋮
2	8	0.166 924	0.166 923 88	0.003 407 99	0.003 409 21
2	9	0.160 179	0.160 178 76	-0.002 842 28	-0.002 849 10
2	10	0.154 172	0.154 172 11	-0.006 976 67	-0.006 972 91
3	0	0.0375	0.037 499 83	0.850 889 57	0.850 888 54
3	1	0.034 375	0.034 374 89	0.646 789 72	0.646 792 39
3	2	0.032 031 25	0.032 031 26	0.430 698 01	0.430 702 05
⋮	⋮	⋮	⋮	⋮	⋮
3	10	0.220 477	0.220 481 21	0.001 313 56	0.001 313 23
3	11	0.213 431	0.213 426 85	-0.006 003 94	-0.006 010 22
3	12	0.207 01	0.207 221 34	-0.011 275 9	-0.011 312 03

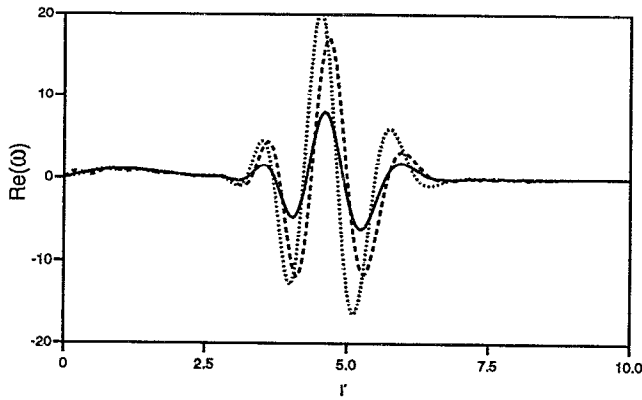


FIG. 2. Real part of the eigenfunctions versus radius for $n=1$, $N=300$, $R=1000$, $k=1$ (solid), 2 (dashed), 3 (dotted).

$$\langle u, v \rangle = \int_0^\infty u \bar{v} e^{r^2/2} r \, dr, \quad (28)$$

such that the coefficients of \mathbf{A} ,

$$\mathbf{A}_{jk} = \langle \omega_j^n(r), \mathcal{L} \omega_k^n(r) \rangle / \langle \omega_j^n(r), \omega_j^n(r) \rangle, \quad (29)$$

can be easily calculated.

By construction, this method reproduces the known eigensolutions for $R=0$. Results for larger Reynolds number are plotted in Fig. 1 for $n=1$. Numerical solutions to (27) were found using the QZ algorithm for values of N ranging from 20 up to 300. For fixed N and n , we find a denumerable set of eigenfunctions and eigenvalues for $k=0, 1, 2, \dots$, each corresponding to a different radial structure of the perturbation. These calculations were tested in various ways. First, for low Reynolds number, our results were compared to and agreed well with the RS results (see Table I and subsequent discussion). Next, for fixed R , the dimension N was increased until convergence was evident. Third, results for Reynolds numbers up to approximately 100 were checked by treating the problem as a nonlinear continuation in the parameter R , starting at $R=0$, using a Newton–Raphson scheme with finite-difference techniques.

RS did analyze the effect of nonzero Reynolds number by way of a perturbation expansion for small R and found that for the eigenvalue expansion

$$\mu = \mu_0 + \mu_1 R + \mu_2 R^2 + \dots, \quad (30)$$

$\mu_0 = n + 2k$ and the coefficients μ_1 and μ_2 were given by RS: {(2.15)–(2.19)}. Since μ_1 is strictly imaginary its value does not affect the stability of the vortex. For low values of k , μ_2 is positive and thereby serves only to increase the value of $\Re(\mu)$. We have calculated μ_1 and μ_2 to larger k than RS, and find that, for fixed n , μ_2 can become negative at sufficiently large k (see Table I). This is equivalent to $(\partial^2 \mu / \partial R^2)_{R=0} < 0$ and indicates a trend toward possible instability at values of R beyond the validity of (30).

Values of $n=1, \dots, 10$ were calculated. In all cases, as illustrated in Fig. 1, $\Re(\mu) > 0$, indicating stability of the Burgers vortex to 2-D perturbations. Note that for values of (n, k) , where (30) indicates $(\partial^2 \mu / \partial R^2)_{R=0} < 0$, we found that $\Re(\mu)$ reached a local minimum followed by a subsequent increase with increasing R . This behavior is on a scale too small to be seen graphically in Fig. 1. Numerical results at high Reynolds indicate that the real part of the eigenvalue grows like the square root of the Reynolds number. The irregularity of the plots at large Reynolds number is caused by resolution problems in representing the vorticity with a maximum number of basis functions, $N=300$.

It was found that, as R was increased at fixed n, k , the eigenfunction became increasingly oscillatory, whilst remaining confined to within a narrow band. This is illustrated in Fig. 2, which shows the real part of the eigenfunction for $n=1, R=1000$. It was this structure that limited the range of our finite-difference method to maximum $R \sim 10^2$ and that of the spectral method to maximum $R \sim 10^4$.

ACKNOWLEDGMENTS

Helpful discussions with P. G. Saffman and D. Crowdy are gratefully acknowledged. This research was partial supported by National Science Foundation Grant No. CTS-9311811.

¹G. I. Taylor, Proc. R. Soc. London Ser. A **164**, 15 (1938).

²J. M. Burgers, Adv. Appl. Mech. **1**, 171 (1948).

³A. A. Townsend, Proc. R. Soc. London Ser. A **208**, 534 (1938).

⁴Z. S. She, E. Jackson, and S. A. Orszag, Proc. R. Soc. London Ser. A **434**, 101 (1991).

⁵A. Vincent and M. Meneguzzi, J. Fluid Mech. **225**, 1 (1991).

⁶J. Jiménez, A. A. Wray, P. Saffman, and R. S. Rogallo, J. Fluid Mech. **255**, 65 (1993).

⁷A. C. Robinson and P. G. Saffman, Stud. Appl. Math. **70**, 163 (1984).